An Analysis of Testing Variables in Rapid Compression Machine Experiments

Jenna Ezzell
Marquette University

AN ANALYSIS OF TESTING VARIABLES IN RAPID COMPRESSION MACHINE EXPERIMENTS

By

Jenna Ezzell, B.S.

A Thesis submitted to the Faculty of the Graduate School,
Marquette University,
in Partial Fulfillment of the Requirements for
the Degree of Master of Science

Milwaukee, Wisconsin
August 2017

ABSTRACT

AN ANALYSIS OF TESTING VARIABLES IN RAPID COMPRESSION MACHINE EXPERIMENTS

Jenna Ezzell, B.S.

Marquette University, 2017

There have been discrepancies noted concerning experimental data from rapid compression machines (RCM). When data is compared from different RCM facilities, the ignition delay times are inconsistent when inspecting any particular temperature. Currently in publications, if these datasets are compared, the discrepancy is said to be due to heat loss, however this issue has yet to be examined more thoroughly. To determine what the root cause of this discrepancy is, four different fake RCM facilities were created and simulated. There were also different sets of initial conditions used to determine how this may affect the data. Simulations were run using a Multi-Zone Model, which is a one-dimensional model that uses a piston trajectory to calculate the change in volume over time to define the pressure in the reaction chamber for a given set of initial conditions. To assist in determining which initial conditions to use for any combination of desired compressed conditions, an Artificial Neural Network was used. A different network was created for each machine, and was trained to be able to predict the compressed temperature and pressure given a set of initial conditions. Once the initial conditions were determined, the simulations were run and the data was analyzed. It was determined that the compression time was the most important geometric factor leading to the discrepancy. It was also determined that the most influential set of initial conditions involved changing the initial pressure of the mixture as well as the compression ratio to reach the desired values.

ACKNOWLEDGEMENTS

Jenna Ezzell, B.S.

I would first like to acknowledge my advisor, Dr. Casey Allen, and my thesis committee, Dr. Simcha Singer and Dr. Anthony Bowman. I would not be where I am today without your guidance. Thank you for taking the time to be a part of this chapter in my life and helping me grow and become a better engineer along the way.

Another crucial component to finishing this project was the friendship and collaboration I received from my research team. Thank you to Jack Rehn, David Wilson, Mark Carioscio, and Ashley Hatzenbihler, your constant positivity and willingness to help with every aspect of the past two years did not go unnoticed. I cannot wait to see where your future ventures lead you.

To the rest of the troublemakers, thank you for forcing me to have some fun every once and a while, and being an understanding and supportive groups of friends to have around through the challenges that getting this degree had to offer.

Thank you to all of my students, for letting me guide you even for a small amount of time during your engineering education. You all challenged me to think outside the box, and helped me to gain a lot of confidence in my engineering skillset, for which I am truly grateful.

To Annette, my “adoptive mother,” thank you for never getting upset when I didn’t know which form to turn in when, for ordering so many of the parts needed in the past two years, and for always looking out for me.

Finally, thank you to my family and friends, near and far, who helped me come out of this experience in one piece. Whether you could fully comprehend the complexity of this project or simply understood the stress that graduate school has to offer, I appreciated you staying by my side through it all.

TABLE OF CONTENTS

LIST OF TABLES

LIST OF FIGURES

Chapter 1: Introduction

Fundamental combustion research has a wide range of testing mechanisms and varying focuses, but can be broken down into three different areas: chemical kinetic mechanisms, chemical ignition studies, and predictive modeling. Chemical kinetic mechanisms are sequences of elementary reactions that represent a global chemical reaction. They are developed to predict what happens during each stage of this complex reaction. The second area, chemical ignition studies, represents the experimental methods used to validate the kinetic mechanisms. Finally, predictive modeling is used to predict chemical behavior and the products of chemical reactions through numerical simulations while using fewer resources than physical experiments. Chemical ignition study experiments are most commonly carried out using one of three testing methods: flow reactors, shock tubes, or rapid compression machines. These methods allow the exploration of ignition properties without the use of an internal combustion engine. The testing method being focused on in this work is the rapid compression machine (RCM). A RCM simulates a single stroke of an internal combustion engine by rapidly compressing a piston into a cylinder containing a reactive fuel and oxidizer mixture. They are designed to aid in the understanding of the low-to-intermediate temperature auto-ignition chemistry under idealized engine like conditions. Most RCMs operate with compression times of 10 to 60 ms, and in an environment that can reach pressures up to 100 bar and temperatures between 600 and 1100 K. Under ideal conditions, all RCMs would provide identical data for similar experiments, however data discrepancies have been observed recently. Most commonly when publishing data, the different RCM facilities simply compare data from their experimental facility to a corresponding model. However, in a few publications, such as one written by Goldsborough [Goldsborough, 2009], there are comparisons made between the data sets of many

RCM facilities. In Figure 1, shown below, there is a clear demonstration of the discrepancy in what should be the same data points from different facilities.

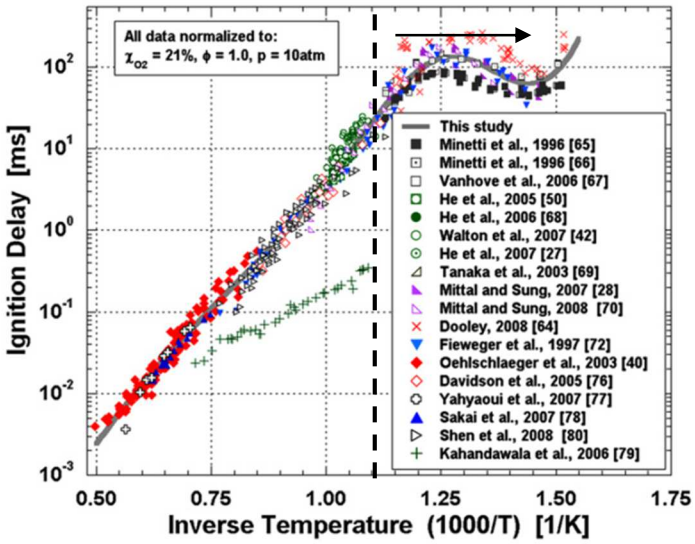

FIGURE 1: RCM DATA FROM DIFFERENT TESTING FACILITIES [GOLDSBOROUGH, 2009]

The data that is on the right of the dashed line represents data taken using a rapid compression machine, as that is the typical temperature range of a RCM. As can be seen, there are approximately six different data sets in the RCM region, with ignition delay times ranging from approximately 800 ms to 5000 ms depending on the temperature. This particular plot was normalized to have the same equivalence ratio, pressure, and amount of oxygen. The normalization of these factors leads to the necessity to explore these differences more thoroughly, as these factors greatly affect ignition timing. However, normalizing these factors also introduces error in the interpretation.

Previously, it has been assumed that these differences are due to heat loss or complex fluid dynamics within the reaction chamber. It is very possible that different facilities have varying amounts of heat loss or differences in the fluid mechanics due to slight physical machine differences. RCMs at different facilities

have many of the same physical components as well as similar approaches to run experiments. While information is typically published disclosing the geometry and setup of an RCM facility when using it for taking data and performing analysis, this is not always the case with how the different facilities obtain their data points. For a given data point, there can be any combination of oxidizer mixture, compression ratio, initial temperature, initial pressure, equivalence ratio, and fuel that is desired. The specific combination of these values may vary between facilities to obtain the same compressed conditions. This could lead to variability between datasets, beyond the obvious physical inconsistencies. To examine both of these hypotheses, it is important to examine both the physical component as well as which combinations of initial conditions lead to which compressed conditions. This is done through the creation of four different "machines". These machines are entirely made up, but based off realistic RCM facilities. Different combinations of initial conditions will also be used to determine how these affect the compressed conditions. The objective of this work is to determine which components of RCM testing have the strongest connection to the data discrepancy.

1.1 Outline

This thesis aims to identify what may be causing this discrepancy. In chapter 2, there is more background information given regarding the purpose of RCMs, typical design features, and the common experimental approach taken. The variances between different RCM facilities are explicitly explained, and the different techniques use to model RCMs are described as well.

Chapter 3 provides details on the model used in this thesis, otherwise known as a multi-zone model. This model was originally developed by Goldsborough et. al [Goldsborough, Banyon, & Mittal, 2012], but was optimized by Wilson et. al [Wilson & Allen, 2016] to the current version used. Chapter 4 explains the setup performed

before the actual simulations were run. To determine which parameter/parameters were most important in the data discrepancy, four different hypothetical machines were “created”. The first of these 4 was based off the RCM facility at Marquette University, and the rest were varied from this base machine by 1-3 of the 5 important parameters selected to be changed. Uniquely simplified velocity profiles were created for each machine due to their differences. These velocity profiles are used as the input to the model. That process is explained in chapter 4 as well as the creation of the artificial neural networks. These networks were created to be able to predict the initial conditions for each machine to meet the desired final conditions.

Chapter 5 displays the results of the simulations and chapter 6 discusses the conclusions and potential future work in this area.

Chapter 2: Background

This chapter discusses the relevant background information regarding rapid compression machines, the geometric and performance variances in the existing RCMs, and the originations of RCM modeling.

2.1 Rapid Compression Machines

2.1.1 RCM design features

There are seven components that can be used to define an RCM as a testing mechanism, and that may vary between facilities. These components are the pneumatic actuation, hydraulic stopping, the orientation of the machine, the piston shape, the compression ratio, the stroke length, and the compression time. The pneumatic actuation is performed using a pneumatic cylinder. The air pressure in this pneumatic cylinder can normally be changed and defines the speed or the driving pressure of the system. The second listed component, the hydraulic stopping, is executed through the use of a hydraulic brake. In the RCM at Marquette University, the hydraulic brake has a stepped down profile, which assists in the process of slowing down the compression towards the end of the experiment. This profile decreases the size internally, so there is more resistance to the movement at that point. The orientation of the machine is typically either right angle or linear. A difference in the orientation allows for different testing efforts and can add some variability to the data points taken. Two examples of different orientations are shown in Figure 2 and Figure 3 below. The RCM displayed in Figure 2 is a top view of the RCM facility at Marquette. The reasoning behind this orientation was to allow for compression as well as compression-expansion tests to be run using different

cams. Figure 3 is the RCM at Case Western Reserve University, and is an example of the classic linear orientation.

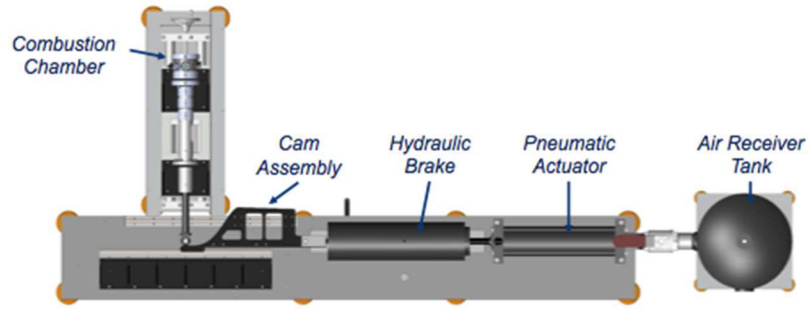

FIGURE 2: MARQUETTE RCM CONFIGURATION [NEUMAN, 2015]

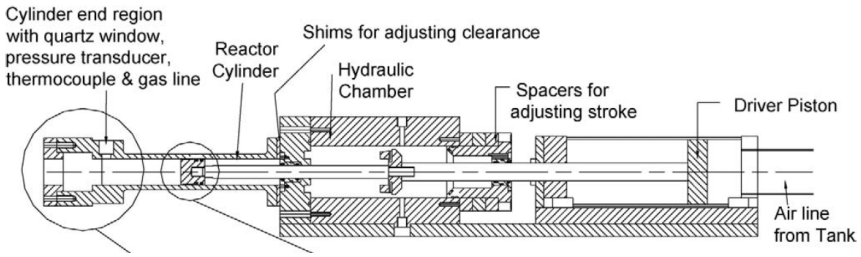

FIGURE 3: CASE WESTERN RESERVE UNIVERSITY RCM SCHEMATIC [MITTAL & SUNG, 2006]

Next, there may be two different piston shapes, flat or creviced. While most RCM facilities use a creviced piston, some still use or have a flat piston. A flat piston is what one would typically assume a piston to look like. The creviced piston was originally developed by Park et. al [Park & Keck, 1990] to counteract a piston-induced vorticular fluid motion within the reaction chamber after the piston had come to rest. Figure 4 below depicts the difference between the flat and the creviced piston. This will be explained more thoroughly in section 2.3, however it is important to note here as well. Essentially, the creviced piston was developed to help simplify the fluid dynamics inside the reaction chamber post TDC, by removing a portion of the piston. While this helps to simplify the reaction chamber fluid

mechanics, it can increase the heat loss during experiments due to the change in the surface area: volume ratio. The crevice design was optimized by Mittal and Sung [Mittal& Sung, 2006]; however, different facilities may change this ratio leading to more or less heat loss.

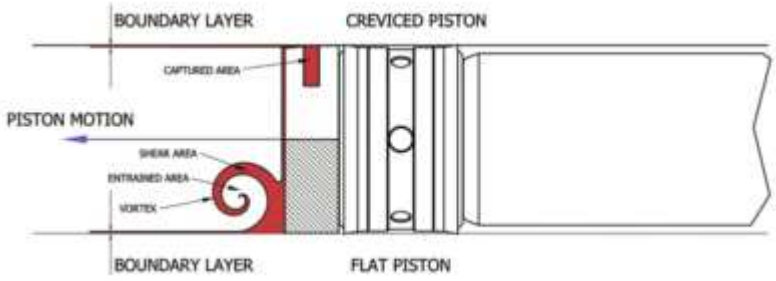

FIGURE 4: FLAT VS. CREVICED PISTON [SUNG & CURRAN, 2014]

The next important component is the compression ratio. This is commonly known as the ratio between the maximum and minimum volume in the cylinder. What is different about RCMs is that this ratio can typically be changed. The reaction chamber of the RCM at Marquette sits on a panel which is attached to a hand wheel. This hand wheel can then be moved to change the position of the reaction chamber relative to the piston, therefore changing the compression ratio. This process will be further explained in the next section. The difficulties with changing the compression ratio include the challenge of accurately describing the change in volume of a small reaction chamber, the different methods that could be used to change the compression ratio, as well as variances in how different testing facilities describe the compression ratio for their machine. Related to the compression ratio is the stroke length, or the length that the piston travels to reach its top dead center position for any given test. The stroke length also closely correlates to the final listed component of the compression time. These two components are closely tied together, especially when it comes to data

discrepancies. A longer stroke length will typically take more time to compress a mixture, allowing more time for heat loss to occur. Similarly, if there is a shorter compression time, this allows less time for heat loss to occur. Most commonly, there is one stroke length and a small range of compression times if there is a range at all. [Affleck & Thomas, 1968; Donovan, He, Zigler, Palmer, Wooldridge, & Atreya, 2004].

From the factors discussed, the piston shape, compression time, stroke length, and compression ratio appear to be most important to this discrepancy. The way these are designated definitely have room for error, especially when comparing different machines. These will be discussed more in the upcoming chapters.

2.1.2 Experimental approach

To understand how there may be discrepancies in different facility datasets, it is important to be aware of what goes into gathering a set of data. While the specifics of different facilities may slightly alter the approach taken experimentally, overall the same initial decisions need to be made when choosing what data points to take, how to maintain consistency throughout a dataset, and the steps taken to run an experiment. The experimental approach taken with the RCM at Marquette will be explained to provide a better understanding of what goes into running a RCM experiment. Parts of this approach may vary with different facilities, however the objectives are the same.

To ensure the accuracy and reliability of the data taken from the RCM, the same procedure is followed for each experiment. There are also some daily calibrations performed including a non-reactive run to ensure machine consistency, checking the fuel injector calibration, and cleaning out the reaction chamber. After the system is turned on and the daily calibrations are performed, the first step is to set the driving pressure or the speed of the system by setting the air pressure in the

air receiver tank. This is done by changing the pressure in the compressed air line attached to the air receiver tank. To verify that the driving pressure is stabilized, there are 2-3 test runs done to make sure that it will not drop lower than the desired pressure. Before these are run, there is also a 15-20-minute wait period to let the air evenly distribute throughout the tank.

After the driving pressure is set, the compression ratio is changed to the desired value by turning the hand wheel attached to the slide that the combustion chamber sits on, as shown in Figure 5 below. The base position was set at a distance of 5 5/8" from the inside of the closest support to the hand wheel on the table. Beyond this position, it was determined that each full rotation of the hand wheel moved the slide 3/16", which was then factored into the volume calculation and therefore the compression ratio at that location. There is a set minimum clearance value to ensure that the piston will not hit the end of the combustion chamber upon compressing. Since a certain number of rotations correlates to a desired compression ratio, this consistent process leads to an accurately determined compression ratio each time.

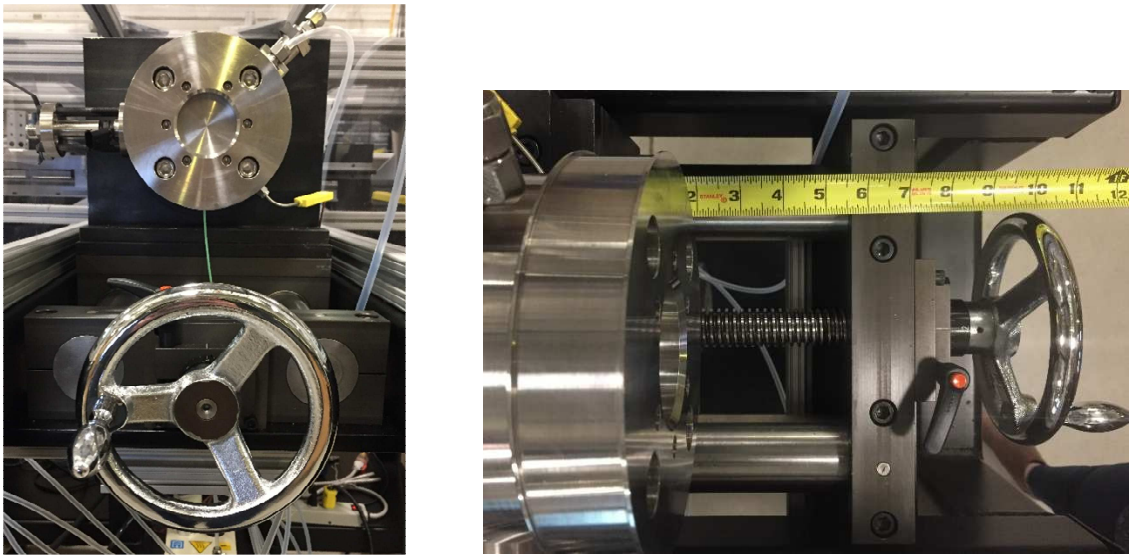

FIGURE 5: FRONT AND TOP VIEWS OF THE MARQUETTE COMBUSTION CHAMBER WITH THE HAND WHEEL

To guarantee that nothing is remaining in the chamber, after the compression ratio is set it is vacuumed out. Once the chamber is vacuumed out, the chamber can then be filled with the oxidizer mixture, assuming that the roller follower is still in its proper position. The oxidizer mixture is filled into the chamber based off the desired pressure. After the oxidizer mixture is in the chamber and the pop-it valve is closed, a set amount of fuel is injected. This is determined by a combination of the equivalence ratio, compression ratio, and initial pressure of the oxidizer mixture. After the fuel is injected, there is a waiting time of 2 minutes to certify that the fuel is all fully evaporated into the oxidizer mixture prior to testing.

While the fuel is evaporating, the rest of the steps needed to perform the experiment are taken. The hydraulic brake is pumped with oil on the backside to 1000 psi to set it before the pneumatic cylinder set-up is pressurized. After the front side of the brake is pressurized, the backside of the piston is drained out

using a three-way ball valve attached to the front of the air cylinder. After this is complete, the ¾-inch ball valve on the rear of the pneumatic cylinder is closed and the three-inch ball valve connecting the driving pressure to the pneumatic cylinder is opened. The three 1-1/2-inch ball valves on the front of the cylinder are then opened to completely arm the RCCEM. It is then confirmed that the displacement sensor is zeroed out as well as the pressure transducer in the combustion chamber before the experiment is run. When the experiment is run, the solenoid valve attached to the hydraulic brake is opened up, draining the oil, and allowing the cam to compress the mixture. The pressure data is tracked through the pressure transducer attached to the combustion chamber.

After the experiment is run, the set-up needs to be reset to the safe position. The safe position allows adjustments to be made if necessary to the cam assembly or the roller follower. This position is when the piston is at a bottom dead center, the valve to the air receiver tank is closed, and the cam is in its initial location. This is done by opening the pop-it valve again using the Charge Preparation VI and introducing approximately 3.5 bar of air pressure into the combustion chamber. The ball valve connecting the air receiver tank to the pneumatic cylinder is closed first, followed by the three 1-1/2-inch ball valves on the front of the cylinder. The ¾-inch ball valve on the rear of the pneumatic cylinder is then opened to vent the air from the front side of the pneumatic cylinder. The three-way ball valve at the front of the pneumatic cylinder is then turned to use the connected air line to pull the cam back to its starting position.

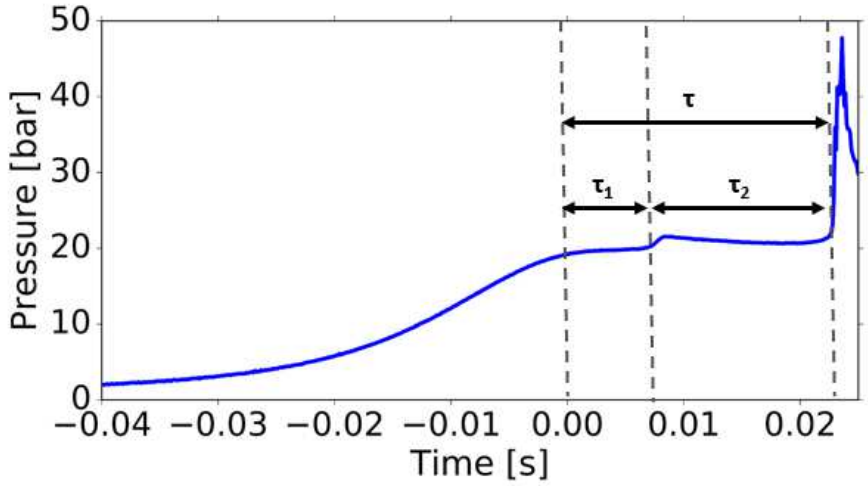

FIGURE 6: SAMPLE EXPERIMENTAL PRESSURE TRACE

Shown in the Figure 6 is typical reactive pressure trace from an experiment. It is common to have a pressure transducer in the reaction chamber to read the pressure during an experiment. From this pressure trace, a compressed or peak pressure can be determined, along with a very common metric known as the ignition delay time. In Figure 6 it can also be noted that the peak pressure is displayed when the time is equal to 0. This is to help simplify and clarify pressure trace comparisons. Out of the different ignition studies testing mechanisms, the rapid compression machine most directly measures the metric of ignition delay time due to the way the data is taken, so it is very useful. As shown in the figure, the ignition delay time represents the time between the peak pressure, when the piston is at top dead center (TDC), and the point of ignition, depicted by the spike in pressure in the figure. Another metric that is known but not always used is the heat release rate. It is not always used with experimental data because it has to be calculated. It can be compared to the change in pressure over time or the derivative of the pressure trace as it represents the amount of heat released due to the reaction at any given time. The most heat release occurs during the actual ignition, as to be expected. This

metric is not as widely used and is difficult to calculate from an experimental standpoint; however, it can be easily determined in a simulation.

2.2 Rapid Compression Machine variances

To help gauge the typical variances between different RCM facilities, there were many resources used. One of the most helpful resources was found in well-known RCM researcher, Guarav Mittal's dissertation. Here he lays out many of the well-known RCMs in a table that clearly shows the differences between certain facilities.[Mittal, 2006] While this is not nearly all of the RCMs being tested throughout the world, it provides an idea for what is specifically different with many of the machines. An image of this table is shown below.

TABLE 1: COLLECTION OF INFORMATION REGARDING DIFFERENT RCM TESTING FACILITIES [MITTAL, 2006]

Affiliation	Driving, Stopping Mechanism	P_{max} (bar), T_{max} (K)	Compression Ratio, Compression Time (ms)	Key Features
Case Western Reserve University	Pneumatically driven, hydraulically stopped	>50 bar, >1100 K (post compression); 350 bar (post ignition)	21 (flat piston) 15.1 (creviced piston), 25-40 ms	Creviced piston, Optically accessible, Specie measurement, Adjustable stroke and clearance
University of Ireland, Galaway	Dual-opposed piston configuration. Pneumatically driven, hydraulically stopped	40 bar, 1060 K (post compression); 135 bar (post ignition)	13.4, < 22 ms	Creviced piston, Adjustable Stroke
University of Leeds	Pneumatically driven, hydraulically stopped	20 bar, 1000 K (post compression)	<14.6, 22 ms	Optically accessible, Specie measurement, Adjustable stroke
University of Science and Technology	Pneumatically driven, stopped by cam	17 bar, 900 K (post compression)	9.8, 20-80 ms	Optically accessible, Specie measurement
MIT (1990)	Pneumatically driven, hydraulically stopped	70 bar, 1200 K (post compression)	19 (flat piston) 10-30 ms	Creviced piston, Adjustable stroke and clearance
MIT (2004)	Pneumatically driven, hydraulically stopped	40 bar, 900 K (post compression)	12.5-16.5, 15 ms	Optically accessible, Adjustable stroke Detachable combustion chamber
University of Michigan	Pneumatically driven, stopped by interference fit of sabot	20 bar, 1000 K (N2), 2000 K (Ar) (post compression)	16-37, 100 ms	Sabot prevents vortex roll-up, Optically accessible, Specie measurement, Adjustable clearance

As previously noted, there are a few similarities between the different facilities such as the fact that of the facilities listed, they are all pneumatically driven, most are hydraulically stopped, and many are optically accessible. However,

when looking at the pressures that can be reached, as well as the compression ratios and the compression times, there is a much wider variety. One of the initial observations made from the differences in these values is that while a shorter compression time may lead to less heat loss, that facility may have difficulties reaching the lower end of temperatures depending on their compression ratio range. These facilities may not all be able to reach the same conditions, or may simply have different methods of getting to the same conditions.

The conditions desired from a given experiment are a particular compressed pressure and temperature. These conditions are used to ensure data consistency, and can be found using many different methods. These methods rely heavily on the RCM testing facility. Some of these may also be more susceptible to issues regarding repeatability, heat loss, or more complex fluid mechanics. Depending on the facility capabilities, it may be possible to preheat the mixture before a test, change the compression ratio, adjust the stroke, vary the clearance, or simply run experiments with a higher initial pressure due to machine capabilities. Preheating the mixture is a facility specific option, which will not only increase the compressed temperature for a given test, but will also affect the compressed pressure. The compression ratio is a commonly changed parameter, which most directly affects the compressed pressure. It is typically not a difficult change to make, and is probably the first option used to change reaction chamber conditions. Adjusting the stroke length and changing the clearance value also relate to this, as they change the surface area: volume ratio. They can most definitely affect the amount of heat loss within a given experiment. While all of these methods can be used to obtain similar compressed conditions, which does not mean the compressed conditions will be the same. Beyond obvious facility discrepancies, the techniques used to obtain these conditions may also be a part of the data discrepancy.

2.3 Rapid Compression Machine modeling techniques

As discussed in the introduction, one of the methods used in fundamental combustion research is predictive modeling. This component of the research is very useful if performed correctly, as it alleviates the need to take data and the predictions are useful to save both time and money. An important element of predictive modeling is the use of chemical kinetic mechanisms. These mechanisms provide the time dependent progression of chemical reactions in a system, consisting of various chemical species and elementary reactions. The specific chemical species and number of elementary reactions in a particular kinetic mechanism vary, however they are all developed to predict the fundamental combustion process.

These kinetic mechanisms are used as part of a larger model to simulate rapid compression machine experiments. While there are many precautions taken to perform experiments in a homogeneous reaction environment, there are always non-ideal effects that need to be accounted for from a simulation perspective. One of the most revolutionary developments in RCM geometries, which greatly affected the modeling process, was the creation of the creviced piston. As previously mentioned, he creviced piston was originally developed to counteract a piston-induced vorticular fluid motion within the reaction chamber after the piston had come to rest. This 'roll-up vortex' increased the rate of transport of energy and mass to and from the cold boundary layer gas out of the 'adiabatic core' of the chamber. The turbulence created in the chamber due to this 'vortex roll-up' increased heat loss, leading to amplified complexity in predicting post-ignition behavior. To counteract this, the creviced piston was developed by removing a small volume from the original flat piston. The purpose of this change was to trap

the cold boundary layer gases from the reaction chamber so the fluid dynamic behavior could be assumed to be laminar or very close to that, and to prevent the cold gases from reentering the reaction chamber during the delay period. This design was optimized and is a very common component in modern RCMs. While the creviced piston reduced the amount of heat loss during experiments, there is still heat loss that occurs due to the change in the surface area to volume ratio. This is one of the most pertinent issues to consider in the discussion of modeling types.

Naturally, one of the first modeling types to come to mind when discussing RCMs is computational fluid dynamics. While this is a very rigorous method and can provide valuable results, it is not the ideal method. This is because running simulations using CFD is computationally expensive. Especially when multiple simulations need to be run the complexity of the set-up and calculations involved is frequently not worth the time. Another modeling approach that has been taken to model RCMs more simply is using a Homogeneous Reactor Model (HRM). A HRM is a representation of an RCM reaction chamber through the use of a single zone with uniform conditions. This method is much simpler than using CFD, however there is additional methodology needed to account for the heat loss, as this model does not account for that on its own.

To account for the heat loss, there are three different methods that can be used, the effective volume approach, a constant volume approach, or a single zone approach using an energy equation. The effective volume approach is a relation that adds on an additional “volume” to represent the heat loss occurring during an experiment. For a given experimental data point, a non-reactive run is performed, and an effective heat transfer coefficient is calculated. Then, after a reactive run is performed, the temperature can be calculated using the pressures and compressed temperature due to an assumption of constant volume. While this methodology is simple, it requires twice the amount of tests, as a non-reactive run is needed for

every desired reactive run. This method has also been found to over predict the heat loss. [Mittal & Sung, 2007] A widely used hypothesis with this approach is the adiabatic core hypothesis. After the addition of the creviced piston to rapid compression machines, it could be assumed that the fluid properties inside the reaction chamber, specifically post TDC could be assumed to be laminar. This hypothesis essentially states that the center of the reaction chamber can be assumed to be adiabatic within a certain region or 'core', with the rest of the chamber being the boundary layer gas. Heat conduction is assumed to be the most influential form of heat transfer in this case, and heat is conducted from the core region to the walls of the reaction chamber. This assumption results in an isentropic expansion of the core gas in response to the heat loss from the boundary layer to the walls. [Mittal & Sung, 2007] There is not any heat loss from the core region, rather the core expands so the pressure of the core and the boundary layer are equilibrated. While this methodology works from an experimental perspective, from a simulation perspective, a pressure profile is needed to properly account for the heat loss. The constant volume approach simulates more of an adiabatic bomb as the reactor physics is not modelled in this approach. The compressed conditions are simulated to obtain ignition, however there is no heat loss with this approach as the chamber is assumed to be adiabatic. This is also a difficult method to validate experimentally as there is no way to avoid all heat loss. The final method mentioned is a single zone approach using an energy equation. This method simulates the affect of a boundary layer on the temperature and pressure of the core gas. It is explained more thoroughly in a paper written by Tanaka et. al. [Tanaka, Ayala, & Keck, 2003]

A technique presented to model RCM experiments using a HRM was a physics-based multi-zone model developed by Goldsborough et. al. [Goldsborough, Banyon, & Mittal, 2012] This approach calculates the pressure profile from an

inputted piston trajectory. This pressure profile can then be used to calculate the desired volume profile for the HRM simulation. This model was later optimized by Wilson et. al, and is the model used in this thesis. [Wilson & Allen, 2016] The specifics of this model will be explained in the upcoming chapter as well as the changes made to the model by Wilson. Essentially, this model is one-dimensional, and splits the RCM into four main sub-models of the reaction chamber, gap, crevice volume, and the ringpack. The reaction chamber sub-model is split into multiple zones, to better model the boundary layer gas related to the adiabatic core hypothesis.

Chapter 3: Multi-Zone Model (MZM)

The original version of the multi-zone model (MZM) was developed by Goldsborough et. al, and optimized by Wilson et. al to the version that is used here as previously mentioned. Original modeling techniques such as computational fluid dynamics, homogeneous reactor modeling, and zero-dimensional modeling are less time and computationally efficient. While concepts from these types of models were useful, the MZM encompasses the necessary components for modeling RCM experiments by making validated assumptions. The following sections discuss these assumptions and a more thorough overview of the MZM, the sub-models within the MZM, and the model validation.

3.1 Overview of the MZM

The multi-zone model was originally developed to account for the heat loss that occurs during the compression process and the delay period. It is a one-dimensional model due to the uniform zone thickness, specifically throughout the reaction chamber, which creates a consistent distance for the thermal gradient. The main four sub-models are the reaction chamber, tapered gap, crevice, and ringpack as shown in Figure 7 below. The reaction chamber is split into multiple cylindrical, concentric zones, each of uniform thickness, to better model the reaction.

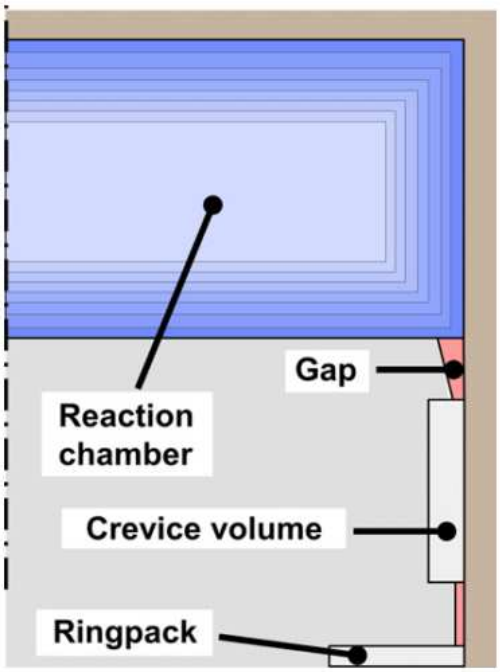

FIGURE 7: MULTI-ZONE MODEL ZONES [GOLDSBOROUGH ET. AL, 2012]

3.1.1 Conceptual Background

The MZM improved previous models by including the adiabatic core hypothesis and the addition of the creviced piston. These two developments create the basis for the zonal breakdown of the RCM combustion chamber and corresponding sub-models. As discussed in section 2.3, the creviced piston was originally developed by Mittal et. al to counteract a piston-induced vorticular fluid motion within the reaction chamber after the piston had come to rest. The adiabatic core hypothesis stems from the simplified fluid dynamics allowed by the creviced piston. This corresponds to the basis of the MZM, as the center of the reaction chamber is assumed to be at a certain temperature, and the surrounding area is broken down into in the aforementioned zones. Heat is conducted between each zone. In the original MZM, the adiabatic core was the only zone where chemistry

was simulated; however, this was changed with the Wilson version. There is no homogeneous reactor model included as each zone has unique and uniform properties.

A simulation models any particular experiment through a given piston trajectory as previously stated. This profile is an input to the MZM, as well as the initial pressure, temperature, and chemical properties based off the fuel and oxidizer mixture used. The piston movement based off the inputted profile volumetrically compresses each zone in the reaction chamber, with conduction between neighboring zones modeled according to Fourier's Law. Mass then flows from the reaction chamber to the crevice through the tapered gap. This flow is driven by the pressure difference between the reaction chamber and the crevice. The crevice is modeled as an unsteady system whose state changes in response to convective heat transfer to the boundary and inlet mass flow from the tapered gap. The ringpack represents the seals typically attached to a piston to prevent the combustion chamber from leaking. This section is modeled to represent any leaks that may occur from the very small space between the seals and the walls of the cylinder. This sub-model was not originally in the optimized model, but was later added on to better represent experimental data.

3.2 Sub-Models of the MZM

3.2.1 Reaction chamber

The reaction chamber is the first sub-model to the MZM and is modeled as a thermally and compositionally non-homogenous mixture where heat is conducted from the adiabatic core of the volume to the colder reaction chamber walls. As discussed in the section above, the core of the reaction chamber is assumed to be adiabatic, with the rest of the chamber being the boundary layer gas. This boundary

layer gas is split into the multiple, concentric cylindrical zones. Each zone is unique in its properties as previously stated, and there is an energy balance for each zone as well. This energy balance includes calculated values such as boundary work, conduction, and chemical heat source/sink terms. It is also important to note that there is no mass exchanged between zones. Each zone is compressed by an amount that is proportional to its size so that the overall volume of the reaction chamber is accurate based off the inputted piston trajectory. A similar approach is taken concerning the pressure for each zone as each zone is compressed or expanded isentropically to equilibrate the pressure in each zone.

3.2.2 Tapered gap

The second sub-model of the MZM is the tapered gap model. The tapered gap is the interface between the reaction chamber and the crevice. As stated above, mass flow is driven by the pressure differential between the crevice and the reaction chamber. This is represented in the momentum equation, which is one of the three balances, as mass and energy balances are also calculated. These three balances are used to calculate the inlet and outlet velocities of the gap, as well as the exiting gap temperature. Due to the coupling of the equations, Newton's method is utilized to take an iterative approach. The input temperature coming from the reaction chamber for forward flow is assumed to be an average of the zone temperatures from the reaction chamber, which was demonstrated to be an accurate through previous CFD simulations where mass was assumed to flow evenly from all zones into the tapered gap. The pressure entering the tapered gap for the forward flow situation can be assumed to be the same as the reaction chamber pressure however.

3.2.3 Crevice

The crevice model is a critical component of modeling the RCM, as it validates the adiabatic core hypothesis through capturing the colder boundary layer gases. This model is treated as an unsteady system whose state changes in response to convective heat transfer to the boundary/wall and inlet mass flow from the tapered gap. There are mass, momentum, and energy balances calculated for this model as well. These calculations are simpler than the tapered gap model however, because the crevice is assumed to have a uniform temperature throughout its volume.

3.2.4 Ringpack

The final sub-model is the ringpack model. This model is assumed to remain in pressure equilibrium with the crevice, due to the volume of the ringpack when compared to the crevice as well as the reaction chamber. The mass flow rate into the ringpack is based off that assumption, while the momentum and energy balances are similar to the crevice balances. Blowby past the ringpack is accounted for by using a quasi-steady, pressure-driven iso-thermal channel flow expression. Due to the size of the gap between the wall and the ringpack, it is also assumed that any gas leaving this volume will come to thermal equilibrium with the wall relatively quickly. This sub-model is important especially from an experimental standpoint because it helps to account for any minor leaks that may occur.

3.3 MZM Validation

3.3.1 Comparison with Computational Fluid Dynamics

The MZM validation for the Wilson version was completed using a comparison to a CFD model. This model created a 30-degree sector of the sub-models described above to simulate the dynamics of the RCM given certain initial

testing conditions. There were three different fuels/fuel-blends, five different compressions ranging from 9-12, and a stoichiometric air to fuel ratio modeled initial conditions. There were laminar flow conditions used as they were previously seen to obtain the best agreement with experimental results. The simulations were all run using the Converge CFD software with the chemistry simulated using the Tsurushima mechanism. The inputted velocity profile was calculated under the assumption that the piston traveled 8 inches in 32 ms, leading to a maximum velocity of 19 m/s. This is also assuming that the cam assembly manufacturing met the specifications.

One of the fuels used in this validation was iso-octane, which is representative of a primary reference fuel. Primary reference fuels are mixtures of iso-octane and n-heptane. Iso-octane represents PRF 100, because the mixture contains 100% iso-octane per volume. The iso-octane tests for the validation at the given conditions were considered to have two-stage combustion where a preliminary heat release event begins and then quickly ceases due to reaction chamber gas temperatures entering and then exiting the Negative Temperature Coefficient (NTC) region. Iso-octane has been thoroughly tested, so this assumption would appear to be accurate.

Figure 8 below displays a set of the conditions run using the MZM with a comparison of CFD simulations run at the same conditions. Overall, there is a strong comparison between the simulations, with a better match occurring at higher compression ratios or shorter ignition delay times. This is common as the longer the ignition delay time, the more complex the dynamics in the reaction chamber become. The largest difference in ignition delay time for any simulation was 6%, which demonstrates an accurate prediction.

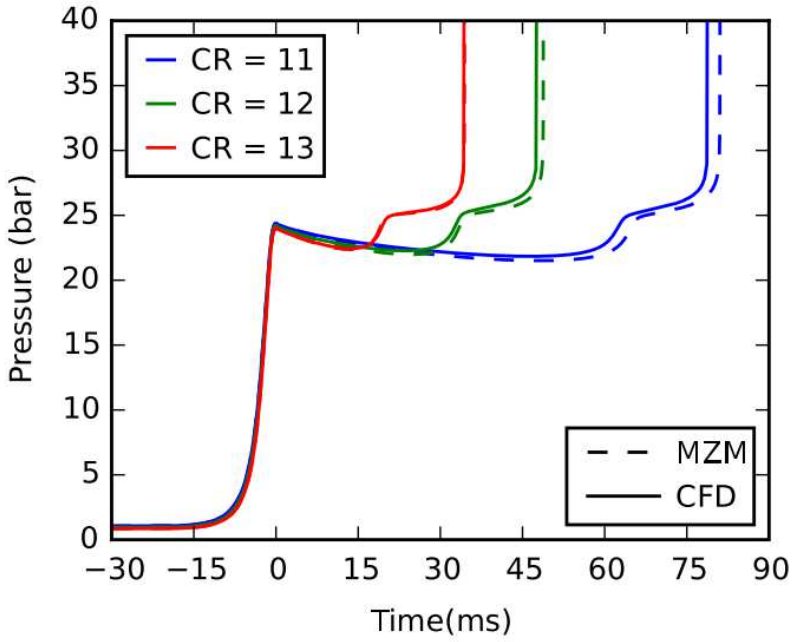

FIGURE 8: MZM VALIDATION WITH CFD [WILSON, 2016]

As previously stated, the Tsurushima mechanism was used for this validation.[Tsurushima, 2009] This mechanism is a more simplified mechanism with only 34 reactions occurring, and was developed to be used to represent primary reference fuel experiments. This mechanism, as well as the mech-ERCPRF mechanism, which is the Engine Research Center PRF mechanism. Using two different mechanisms for the simulations help to provide a frame of reference for how accurate the mechanisms are, and to help represent variability in the kinetics.

Chapter 4: Simulation Set-up

As previously stated, the objective of this research was to determine which parameter most greatly affects the data discrepancy between different RCM facilities. This was done by creating four simulated machines, each representing different potential RCM facilities. However, only one of these simulated machines was modeled after a real RCM. The real RCM it was modeled after is the one at Marquette University. The other three "machines" were varied by one to three of the possible five parameters to be able to specifically determine which parameter created the largest discrepancy. To be able to simulate these different RCM facilities, a uniquely simplified velocity profile was created for each one as described in section 4.2. This third sub-section of this chapter discusses the set-up and execution of an artificial neural network for each of the machines. These networks were used to find the initial conditions for each machine to reach the desired final conditions.

4.1 Machine geometries

To demonstrate the differences between different RCM facilities, there were four fake machines "created" to simulate as shown in Table 2 below.

TABLE 2: TABLE OF SIMULATED MACHINE GEOMETRIES

Machine Geometries	Base case	Crevice volume*0.5	Faster compression time	Larger bore
	1	2	3	4
Compression ratio range	6 -> 13	6 -> 13	6 -> 13	5 -> 15
Stroke length range	8"	8"	8"	8"
Crevice volume	5.51E-06	2.75E-06	5.51E-06	8.30E-06
Bore diameter	2"	2"	2"	3"
Compression time	30 ms	30 ms	15 ms	30 ms

The first of these, as stated above, was based off the RCM facility at Marquette. The other three were changed based off five different parameters. The values highlighted in green in the table were the values that were changed from the first simulated machine, which was the one representing the Marquette facility. While the goal was to only change one parameter per each new machine simulated, some of the changed parameters affected the others, leading to more than one being changed for some of the machines. The parameters altered were the compression ratio range, the stroke length, the volume of the crevice, the diameter of the bore, and the compression time. Since the heat loss and the fluid mechanics were two reasons previously given as hypotheses regarding why the data discrepancy has been occurring, these parameters were chosen to try to highlight what may be causing them. Heat loss commonly occurs in RCMs which have longer compression times and a higher surface area to volume ratio. The crevice volume can affect the heat loss due to the fact that there is a change in the surface area to volume ratio. The compression times create variability in the amount of heat loss. The longer the compression time, the more likely there is to be heat loss in the system. The fluid dynamics is not as complex due to the addition of the creviced piston to the

geometry; however, certain experimental conditions may cause some variability. The RCM facility at Marquette, known as machine 1 for the sake of the simulations, has a compression ratio range of 6 – 13 to be within the desired temperature range and desired minimum clearance of 0.5". This clearance was determined based off what was safe experimentally to ensure that the piston would not hit the back end of the combustion chamber as well as to avoid a high surface area to volume ratio. This minimum tolerance was carried throughout the different machines to simulate realistic conditions. The stroke length was determined by the height of the compression portion of the cam on the RCM. Figure 9 below provides a more clear demonstration of the stroke length metric. This figure is specific to the RCM facility at Marquette, where the 8" measurement represents the stroke length.

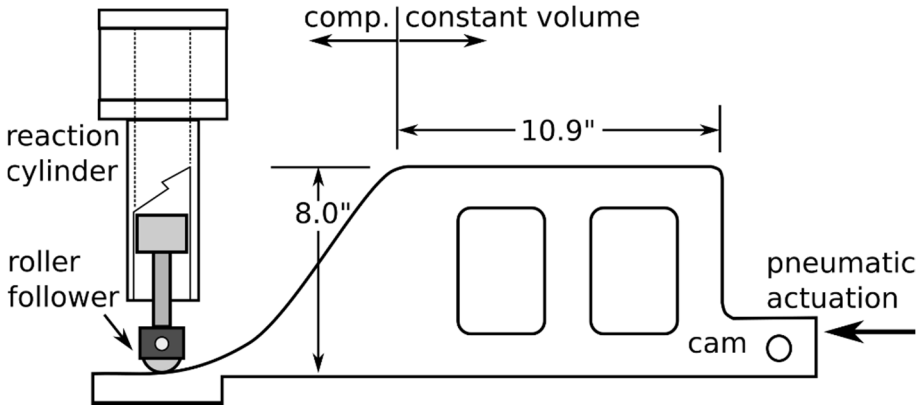

FIGURE 9: SCHEMATIC OF THE CAM OF THE RCM

The crevice volume was calculated based off the specific geometry of the machine. The main purpose of this crevice, as discussed above, is to pull off the cool gases from the reaction chamber to simplify the fluid dynamics inside the reaction chamber as well as to create conditions that would allow for the use of the adiabatic core assumption. The bore diameter is similar in most RCM facilities, which carried over to the changes made in the simulated machines. This parameter had an effect on the crevice volume due to the connection between the piston

volume and the bore diameter. This was the reason behind the crevice volume changing along with the bore diameter. These changes also led to the need to change the compression ratio range, which demonstrates the importance of the crevice volume parameter. The final parameter that was varied was the compression time. This affects both the heat loss component and the fluid mechanics. Shorter compression times decrease the possibility of heat loss due to having less time to lose heat.

4.2 Piston Velocity Profiles

For each machine to be accurately represented in the MZM, there needs to be a different velocity profile. From previous work done, there was a method used to simplify an experimental displacement profile to obtain an accurate depiction of the corresponding velocity profile. These velocity profiles were created based off an assumption that there would be an increase in velocity over a period of time, a small time period of constant velocity in the middle of the profile, and a deceleration to a velocity of zero at the end of the compression stroke. These three sections are the basis for the creation of the profile. The maximum velocity is assumed to be the constant velocity for the profile approximation. The acceleration and deceleration slopes are based off the assumed inflection points in what would be the acceleration profile. An example of this concept is explained in Figure 10 below. There are four important selected times for this simplification, the inflection points where the acceleration would be zero, and the times where the slopes of the acceleration and deceleration values are equal to the constant velocity portion. There is an actual experimental velocity profile also depicted in this figure to demonstrate how this idea originated. This process was simplified when making arbitrary profiles, however the conceptual basis is still the same.

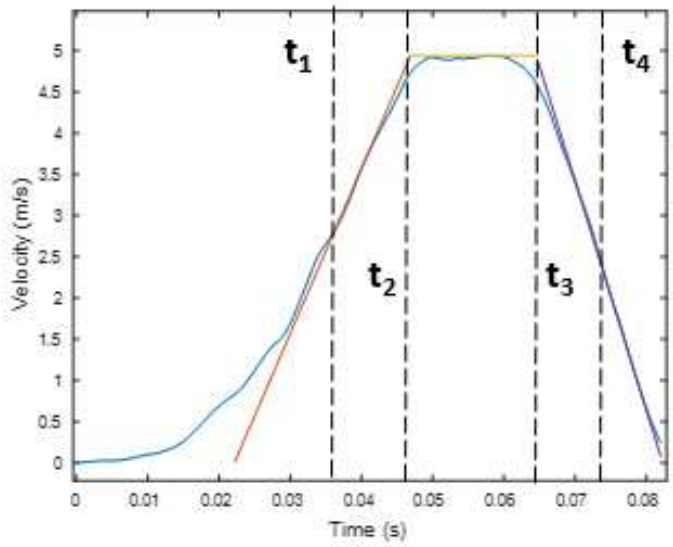

FIGURE 10: VELOCITY PROFILE EXPLANATION

There are two important parameters from the machine specifications that need to be met, the stroke length and the compression time. The compression time represents the total time for the velocity profile to go through the stages of acceleration, constant velocity, and deceleration to get to a velocity of zero at the end of compression. Once the compression time was achieved, the stroke length needed to be included. To check that the piston movement represented the proper stroke length, there was an integral taken over the velocity profile after it was created to convert it to the maximum displacement value. This maximum displacement value directly correlates to the stroke length. Based on if the specifications for stroke length were met, the maximum velocity was either increased or decreased and the acceleration and deceleration curves slopes changed to match that until the proper value was reached. An example of a final velocity profile used is shown in the Figure 11 below.

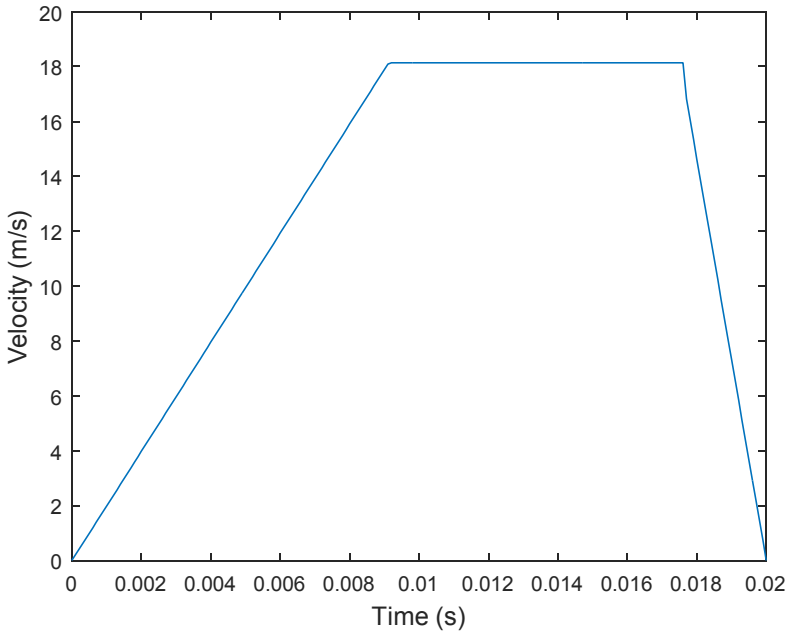

FIGURE 11: SIMULATED VELOCITY PROFILE

4.3 Artificial Neural Network

The simulation conditions led to a total to 21 conditions to be run per machine, as shown in the first column of the Table 3 below. Having a large number of conditions introduced the challenge of having to determine initial conditions that would meet specified tolerances for each RCM.

TABLE 3: SIMULATION TESTING CONDITIONS

Test conditions	
Set conditions within a certain tolerance	Changing initial conditions
$\Phi = 1$	% Ar = 0 - 60
PRF = 100	T_0 = 300 – 450 K
P_C = 20 bar	P_0 = 0.5 – 2 bar
T_C = 600, 650, 700, 750, 800, 850, 900 K	CR range

To help determine which initial conditions to choose for the final simulations, an artificial neural network was created. An artificial neural network (ANN) is a computing system based off the biological neural networks of animal brains. These systems "learn", or progressively improve their performance to give input-specific outputs. They are trained with a training data set of known inputs and outputs, and then can be used to determine unknown outputs from a set of given inputs. Based off the inputs, there are "signals" sent through hidden nodes and the trained network to determine the proper output based off the given information. There are a few factors that affect the accuracy of the network; the number of hidden nodes, the size of the training data set used, and the training algorithm implemented to list a few. There were 15 hidden nodes used, which was sufficient, and the training data sets per machine usually consisted of 500-700 simulations. The training data set is the most important parameter of those listed. An insufficient data set size cannot be trained well no matter the number of hidden nodes or the algorithm used. There was an ANN created for each machine with the initial temperature, initial pressure, compression ratio, percentage of argon, equivalence ratio, and PRF number as the inputs. From these given inputs, the compressed temperature and pressure were outputted. The ANN is helpful to resolve the challenge of determining which changing initial conditions to use for particular outputs. An iterative process can be used by guessing the initial

conditions that will meet the desired compressed conditions. This process will be outlined more specifically below.

4.3.1 Training data

Each machine needed a specific training data set. The training data set needed to be representative of all of the conditions that were desired, so the trained ANN could accurately predict in those ranges. The training data simulations were performed with the chemistry in the model turned off because the only desired outputs were the compressed conditions. The planned outputs of the ANN were the compressed pressure and temperature. These conditions occur when the piston has reached top dead center, therefore, the training data simulations only needed to be run until TDC was reached. The inputs for these simulations are the other six values listed in Table 3.

The equivalence ratio and fuel composition values most directly affect the chemistry. The equivalence ratio represents the ratio of actual air/fuel ratio to the stoichiometric air/fuel ratio. A primary reference fuel was used for these simulations because PRFs are well-characterized fuels. There was only one combination of fuel and equivalence ratio chosen due to the desire to gain an initial understanding of this discrepancy.

The percentage amount of argon and the initial temperature of the mixture have the strongest effect on the temperature of the mixture. The percentage amount of argon in the oxidizer mixture is based off an initial assumption that there is always 21% of oxygen in the mixture. In a mixture with no argon, the oxidizer mixture would consist of 21% oxygen and 79% nitrogen, or just air. Changing the amount of argon in the mixture allows for variability in the temperature of the mixture, as the more argon, the more reactive the mixture is and the higher the temperatures that can be reached. The other factor that will change the temperature

of the mixture is increasing the initial temperature of the mixture. This is not a capability of the RCM at Marquette, but it is simple to preheat the chamber. Many real RCM facilities have this capability and that is why it was chosen as a factor to be changed for these simulations.

The final two factors, initial pressure and the compression ratio range, have the largest effect on the pressure of the mixture. The peak pressure of the reaction is directly proportional to the initial pressure; a higher initial pressure will lead to a higher peak pressure during the reaction. The range of 0.5 – 2 bar was chosen from experimental work done on the RCM at Marquette. This range is standard among RCMs and was the same for all of the machines. The compression ratio, or the ratio of the maximum to minimum volume in the cylinder, varied from machine to machine. As previously stated, a minimum clearance value of 0.5" from the back of the reaction chamber was decided upon to prevent the piston from potentially hitting the back of the reaction chamber in a real experiment. Therefore, with a longer stroke length, there was an added capability to increase the compression ratio range as well as a varied surface area to volume ratio.

Once the conditions were decided upon, the training data simulations were set-up. This was done by creating different codes for each machine to verify that the training data fit that machine's geometry. The equivalence ratio, PRF number, initial pressure, initial temperature, percent argon, and compression ratio were all randomly sampled within the specified ranges above to ensure that peak pressure and temperature conditions were met. To ensure that there were enough training data points, there were 1500 simulations run per machine. It was also assumed that not all 1500 simulations would run due to the fact that the initial conditions were being randomly sampled and some combinations would not lead to convergence. This is because the random samples may not be logical as combinations, leading to issues with the physics of the model. The output of all of these simulations

included all of the initial conditions as well as the time, the pressure in the reaction chamber at each time step, and the temperature in the reaction chamber at each time step to use as the training data.

The outputs of the simulations were then checked to verify that the compressed conditions were in the ranges desired and organized in a way to ensure that the ANN was created as intended. Figure 12 and Figure 13 below show one of the training data sets resulting compressed pressure and temperature sets. It can be observed that the training data set clearly covers the desired ranged of 10-30 bar for the compressed pressures, and 600 – 900 K for the compressed temperatures. It is also acceptable that some of the data goes outside of those ranges, as that is just additional data.

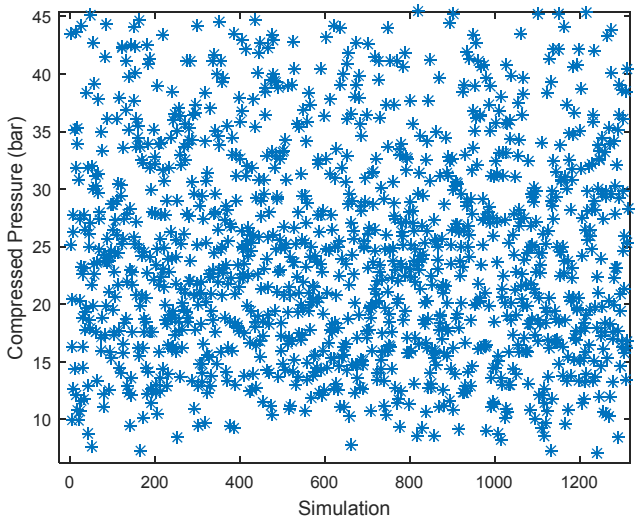

FIGURE 12: COMPRESSED PRESSURE SAMPLE TRAINING DATA

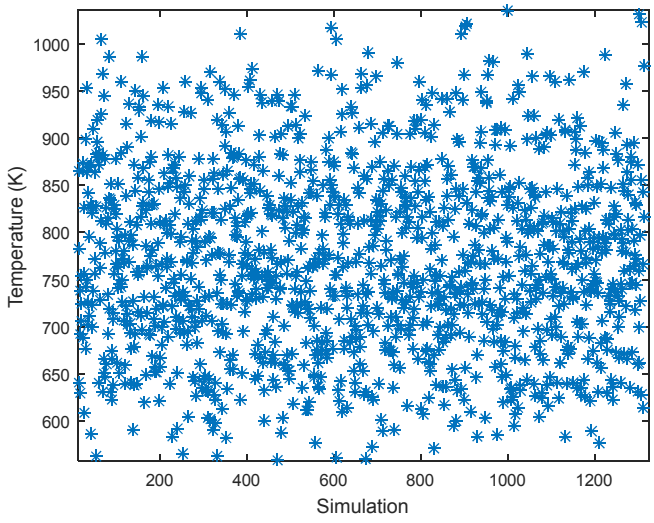

FIGURE 13: COMPRESSED TEMPERATURE SAMPLE TRAINING DATA

4.3.3. ANN accuracy

To set-up the ANN, the data from the simulations mentioned above was used to train the ANN, and the accuracy of the ANN could be seen to determine whether it needed to be retrained or just trained differently. The idea behind the use of the ANN for the real simulations was that a guessed set of initial conditions could be inputted into the ANN, and the compressed pressure and temperature would be outputted. It could then be determined whether these conditions would likely work or not by comparing them to the desired compressed conditions for those initial conditions. If the outputted values were within a particular tolerance, the initial conditions would be accepted, if not, the guesses for the variables, which were changing, were iterated until the method converged. The tolerances selected were 0.2 bar for the peak pressure and 10 K for the temperatures. These values are logical, especially when compared to the desired values. The goal of the ANN was to reach convergence within the specified tolerances. Therefore, in the setting up of

the ANN, the initial pressure, initial temperature, percent argon, compression ratio, equivalence ratio, and PRF number from the training data were the inputs, while the compressed pressure and temperature were the outputs. It was trained using the Levenberg-Marquardt algorithm. This algorithm automatically stops when the generalization stops improving, which is indicated by an increase in the mean square error of the validation samples. Essentially, this means that when the error is minimized based off a calculated RMS error the algorithm will stop running and output those values. Of the data inputted for training, 70% is used to train the network, 15% is allocated for validating the network, and the other 15% is used to test the network and ensure its accuracy. The number of hidden nodes or neurons can also be selected and was chosen to be 15. Since the amount of training data was quite large, this hidden neuron number was not as crucial, but still important to consider.

After the network was trained, there were two plots generated to depict the accuracy of each ANN. The first of these is the regression plot. This plot represents the training, validation, and testing stages of the neural network creation relative to a linear fit, which represents a strong correlation and an RMS error of one, which is the desired value. This is not always achieved with a regression plot for one of the neural networks is shown in Figure 14 below.

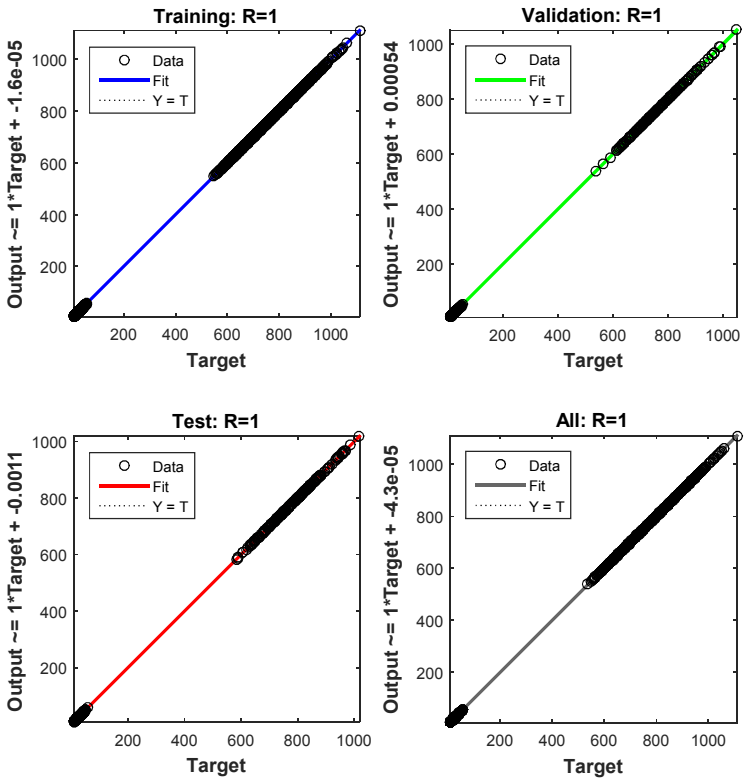

FIGURE 14: MACHINE 1 NEURAL NETWORK REGRESSION PLOT

From this figure, the RMS error is equal to one representing a solid training data set and an overall strong neural network. The data points represent the compressed pressures and temperatures, hence the large gap in the data as those particular values are not very close to one another. The other important plot generated is the performance of the neural network. This figure represents how well the neural network performed through each iterative training of the neural network otherwise known as an epoch. An epoch is a single pass through the entire training set, followed by the testing of the verification set. As shown in Figure 15 below, machine 1 took 1000 epochs to see a solid performance.

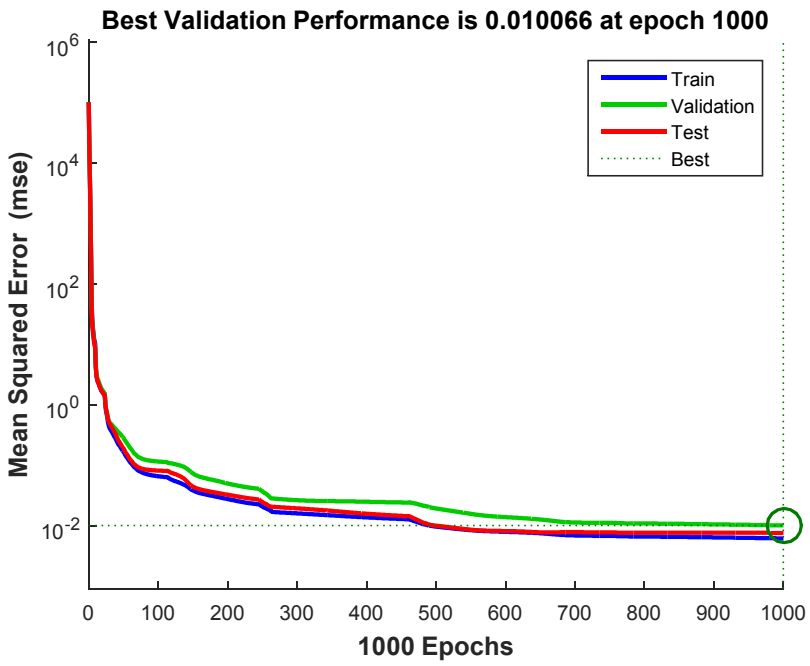

FIGURE 15: MACHINE 1 NEURAL NETWORK VALIDATION PERFORMANCE

Overall, the neural networks for each machine were demonstrated to be accurate and ready to be used to predict which initial conditions for the real simulations.

4.4 Simulation conditions

The real simulation conditions were discussed above, and the neural networks were created to determine the initial conditions to be used for each set of desired output conditions. The last portion of preparation to note before discussing the results in chapter 5 is the methodology used to pick the initial condition combinations. As previously mentioned, the training data sets for each machine randomly sampled all notable parameters within the desired ranges. This could potentially involve a high initial temperature, a low initial pressure, any form of equivalence ratio, a high percent of argon, or a low compression ratio. Not only

does this create a situation where it is unclear which parameter is the most important regarding the output, but it is unrealistic in an experimental setting to change so many parameters at once. To prevent this from happening but to also be able to reach the desired conditions, three cases were run through the ANN to determine which situation would lead to the most accurate final conditions, while keeping some parameters consistent.

TABLE 4: INITIAL CONDITION COMBINATIONS

Case 1	Case 2	Case 3
$T_0 = 300$	$T_0 = 300 - 450$	$T_0 = 300$
% Ar = 0.0	% Ar = 0.0	% Ar = 0 - 60
$P_0 = 0.5 - 2$	$P_0 = 0.5 - 2$	$P_0 = 0.5 - 2$
CR -> changing within machine range	$CR = (C_{min} + C_{max})/2$	$CR = (C_{min} + C_{max})/2$

The three different cases used are shown in Table 4 above. For each case, 2 of the 4 parameters were kept constant while the others changed within the known ranges. Each case was run through the neural network for a given φ, PRF, P_C, and T_C, as listed in Table 3. Ideally, all of the conditions could be met using all of the cases, but that is not physically possible. To determine the initial conditions for a given case, there was an initial guess made as the set of initial conditions, these conditions were then inputted to the ANN for that machine, and a P_C and T_C combination was outputted. If the outputted values were within the tolerance of the desired values, that set of initial conditions was outputted and used for the simulation. If it was not within the tolerance, the initial conditions were continuously changed based off the case being run until it converged to an output within the tolerance. The cases described above have two changing parameters and two constant parameters. The two changing parameters also have ranges that they

need to stay in based off the trained neural networks. This is where the limitation comes in as to which cases can be used for meeting desired conditions. When changing the initial pressure and the compression for case 1, this can only reach temperatures in the lower range. The second and third cases introduce a heating component through the use of either preheating the mixture or introducing argon into the oxidizer mixture. These two cases may not work for the lower temperatures but should be able to reach the higher ones. These physical restrictions seem logical, and a variation should be seen in the data. It is also important to note that all of these cases should ideally reach the exact same compressed conditions and have the same ignition delay time, however this may not be the case.

Chapter 5: Results

The simulations were run for the conditions above and the results are shown in this chapter. The metric used to relate the simulations was the ignition delay time that was previously described. The data from different machines was compared, and the different initial condition cases used to reach these conditions were also analyzed.

5.1 Machine performance

The first important aspect to analyze is the different machines and how they performed. Then the results from all of the machines can be compared to make observations.

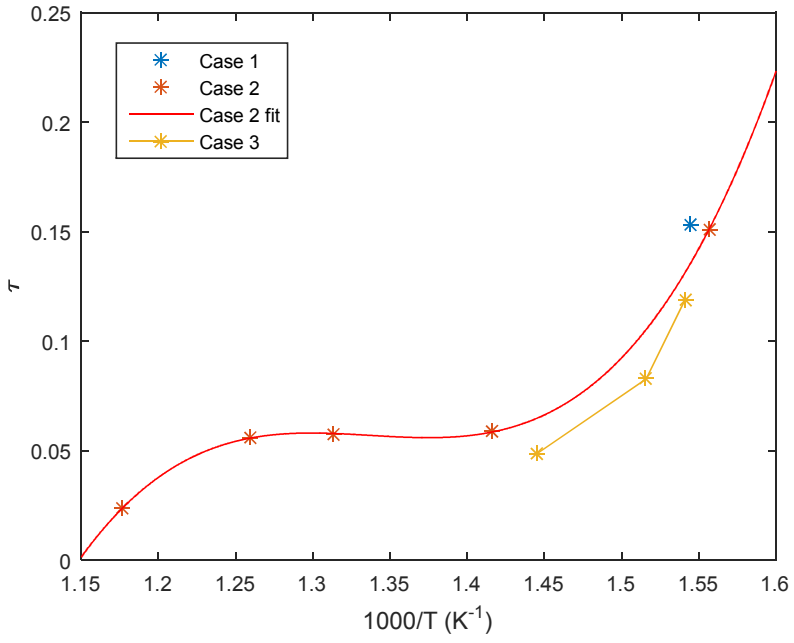

FIGURE 16: MACHINE 1 DATA

Figure 16 above shows the delay time versus 1000/T for the first simulated machine. The initial condition cases are noted with the first case being the compression ratio change, the second case being the initial temperature change, and the third case being the amount of argon in the oxidizer mixture changing. The first and third cases do not span the temperature range due to the limitations of the cases. This can lead to non-reactive runs, especially for the lower compressed temperatures. For the first case where the compression ratio is changed along with the initial pressure, there is only one data point depicted. The reason this occurred was twofold. The lower compression ratio changes did not lead to high enough temperatures and pressures for the mixture to react. Any points that may have occurred at higher compression ratios were not tested. This is due to the methodology used to determine the initial condition values using the neural network. This method would not converge to a set of compressed conditions that was not within the desired tolerances. These values most likely did not reach the desired compressed conditions. The second case spans the most temperatures and gathers most of the desired trend. The trend to be expected for any RCM data set is a decrease in the ignition delay time until about 700/750 K where the delay time increases slightly before decreasing again. This area of the curve represents what is known as the negative temperature coefficient region. [Curran, Gaffuri, Pitz, & Westbrook, 1998] The NTC region represents a temperature range where the ignition delay time of a fuel-oxidizer mixture increases as the temperature increases. This region divides a zone of low-temperature kinetics from a one of high-temperature kinetics. It can be seen that the case 3 or the argon case predicts shorter ignition delay times overall.

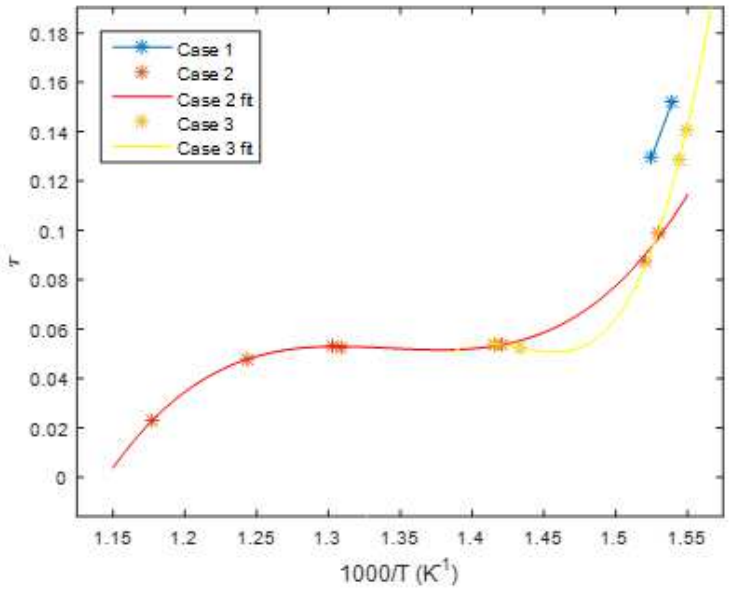

FIGURE 17: MACHINE 2 DATA

The 2nd machine data is depicted in Figure 17 above. This machine covered more data points than the first, which demonstrates a difference in the machine testing abilities due to the crevice volume change. By decreasing the crevice volume, the surface area to volume ratio relating the crevice volume to the reaction chamber decreases, thus limiting the flow that can enter the crevice. The trend is again seen to be different for cases two and three especially as the limited amount of argon that could be added into the oxidizer mixture was not enough to reach the higher temperatures. Case 1 demonstrates longer ignition delay times, which makes sense, as the physics of changing the compression ratio is different from increasing the initial temperature of the mixture or adding argon.

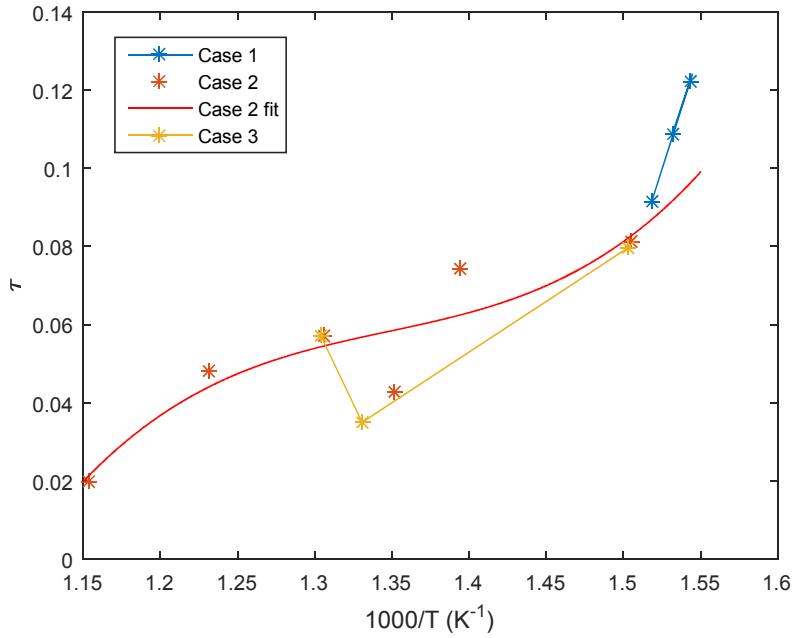

FIGURE 18: MACHINE 3 DATA

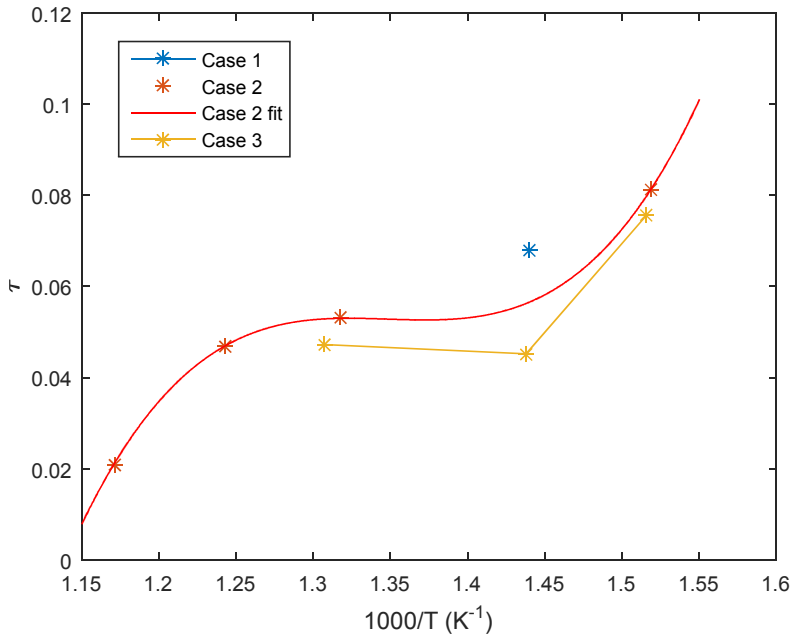

FIGURE 19: MACHINE 4 DATA

Machines 3 and 4, with data shown in Figure 18 and Figure 19 above. Overall, the initial conditions used to simulate the experiments definitely seem to be important as the delay time varies at any given temperature due to using a different set of initial conditions. This is important to note moving forward, especially when comparing the machine data sets to each other. The other trend noticed was that case 1 could only be used to simulate the lower compressed temperatures, case 2 was mostly intermediate temperatures, and case 3 worked mostly for the higher temperature cases. This is to be expected to a certain extent considering how the cases are set-up. Each initial condition has restrictions on how much the varying value can be changed. These limitations were set based off typical experimental ranges. The compression ratio ranges change based off the machine geometries. This limitation was set under the assumption that the operating conditions would be realistic for these machines. The minimum compression ratio for a given range is not as important; however, the maximum compression ratio is a limited parameter. The maximum compression ratio for a given machine is set based off the minimum clearance desired for that machine as well as the surface area to volume ratio at that compression ratio. This surface area to volume ratio in the reaction chamber is very important in relation to the amount of heat loss from that machine. The initial conditions for the pressure and temperature were limited to realistic experimental conditions as well. For the amount of argon in the mixture, there was a maximum amount desired for the properties of the gas. All of these conditions were changed one at a time to simplify the analysis and to be able to easily identify which initial condition case was most impactful.

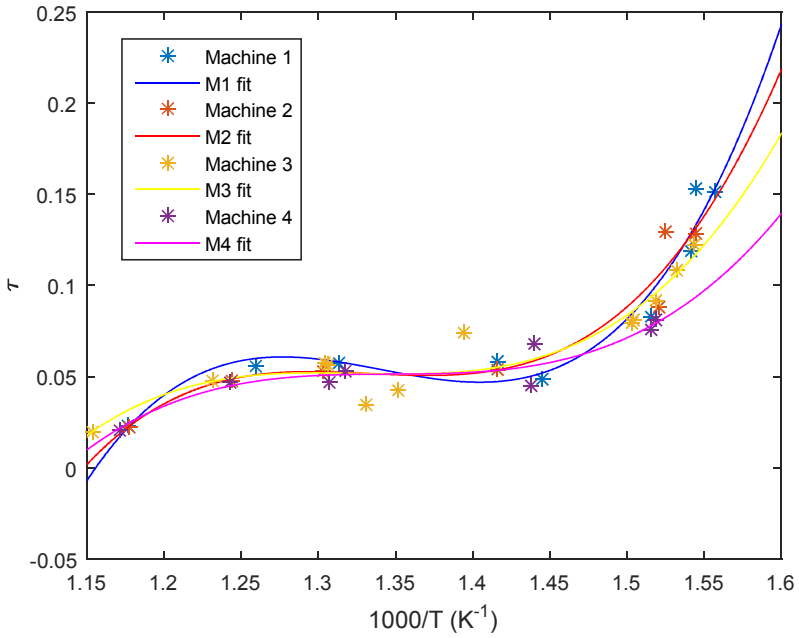

FIGURE 20: MACHINE DATA COMPARISON

Figure 20 compares all of the data points from every machine. It can be seen that the data sets are not the same as the ignition delay times vary within a given compressed temperature value. The 1st machine is considered the base machine as that was the one that was not changed at all and modeled the real RCM facility at Marquette. From this figure, certain areas were highlighted where different delay times occurred from different machines at the same temperatures at 650 and 750 K. The purpose of this was to determine which machine varied the most and why that may be.

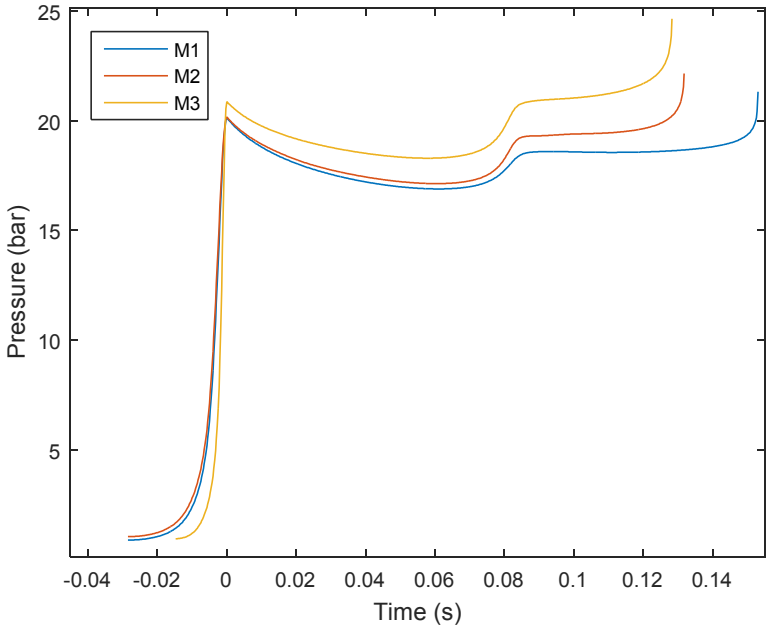

FIGURE 21: 650 K (+/- 5 K) COMPRESSED TEMPERATURE DATA POINT COMPARISON

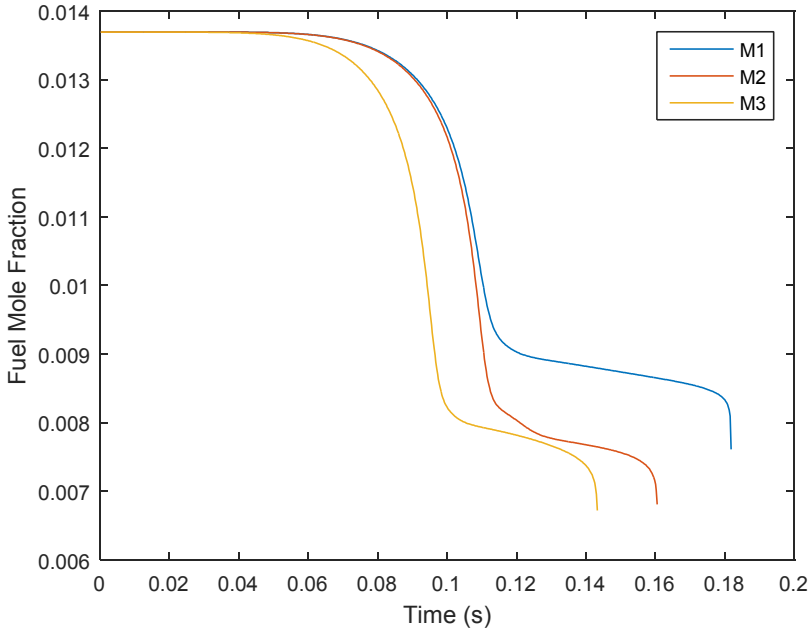

FIGURE 22: 650 K FUEL CONSUMPTION DATA POINT COMPARISON

Figure 21 and Figure 22 above depict data points taken from different machines that ideally represent the same compressed temperature. Figure 21 shows the pressure traces of each data point, taken from machines 1, 2, and 3. The ignition delay time for machine 1 is the longest, while machine 3 is the shortest. Within the overall delay time, it is important to note the characteristics of the first and second stages. The first stage represents heat release and any heat loss in the reaction chamber after reaching top dead center, as well as the loss of pressure due to the amount of mixture flowing through to the crevice. The most heat loss/crevice flow can be seen in machine 1. Machine 2 has less due to the decreased crevice volume, which decreases the surface area to volume ratio. By decreasing this ratio, there is potentially less heat loss to occur as previously noted. The third machine has the least amount of heat loss/crevice flow, and has the shortest first stage of ignition. The third machine had a compression time of 15 ms, which was half of the other two machines that had compression times of 30 ms each. This creates less time for the heat loss and crevice flow to occur. This also creates a higher pressure in the reaction chamber with less time to compress the mixture, and leads to the shortest ignition delay time. It is important to note as well that a given amount of crevice flow will influence the pressure profiles for each machine differently due to the difference in the reaction chamber volumes. Figure 22 is a further investigative component to see how the amount of fuel in the reaction chamber at a given time changes. As Machine 3 demonstrates the most rapid fuel consumption, this correlates to the shortest ignition delay time. This may be due to the shorter compression time or the fact that argon was introduced into the mixture.

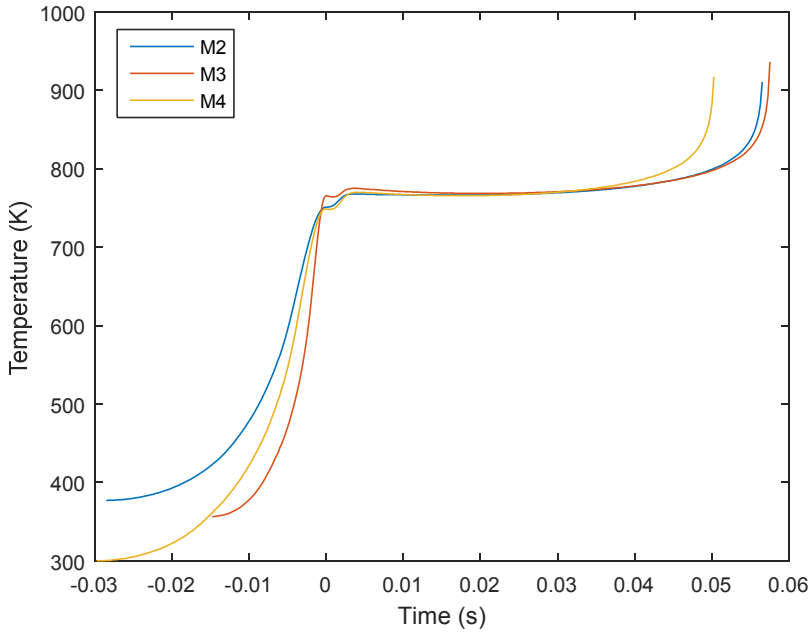

FIGURE 23: 750 K(+/- 5 K) COMPRESSED TEMPERATURE DATA POINT COMPARISON

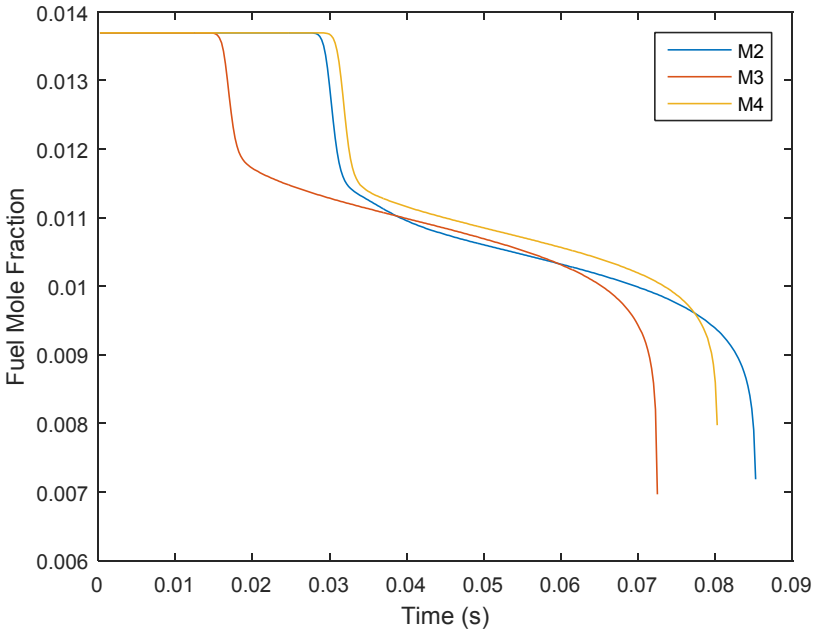

FIGURE 24: 750 K FUEL CONSUMPTION DATA POINT COMPARISON

Figure 23 and Figure 24 represent data points chosen at 750 K. These data points were taken from machines 2, 3, and 4. Figure 23 represents the temperature within the reaction chamber during an experiment. It was decided to examine the temperature curves as opposed to pressure for this set of data points because 2 of the 3 initial condition cases chosen were the second case, where the initial temperature was increased. The other case, which is represented through the curve for machine 4, was the third case where argon was introduced into the oxidizer mixture. Two main things to note from this figure are the fact that the ignition delay time for the third machine is longest here, and that the delay time for the fourth machine was the shortest. The change made for the fourth machine was a larger bore diameter. With the larger bore diameter, the crevice volume is also increased. With an increased crevice volume it would be assumed that there would be more flow to the crevice and more heat loss after the piston reached top dead center, this would be assumed to have a longer ignition delay time. However, this is where the importance of the initial condition cases used becomes substantial. The reason that the ignition delay time for the data point from the fourth machine is shorter than the third machine data point could be due to the machine geometry differences or because of the initial condition case used. For the data point pulled from machine 3, the second case, or initial temperature change case was used. For the data point chosen from the fourth machine, the third case or the amount of argon in the oxidizer mixture increasing was chosen. With the other two data points, the second case was used, so the initial temperature was increased to reach the desired compressed conditions. While this can decrease the ignition delay time when compared to only changing the compression ratio, it does not affect the mixture enough to ignite as quickly at a given temperature as a mixture with argon present. The other figure, Figure 24 validates this, as the fuel consumed during the

first stage for the third machine is still the quickest, but the 4th machine has the argon present to change the thermal properties of the mixture.

5.2 Initial condition analysis

The second component to this analysis was determining the effect of the initial conditions on the outputted data. The cases were compared for all of the machines, as well as particular data points chosen within the same machine to see how they can change the data.

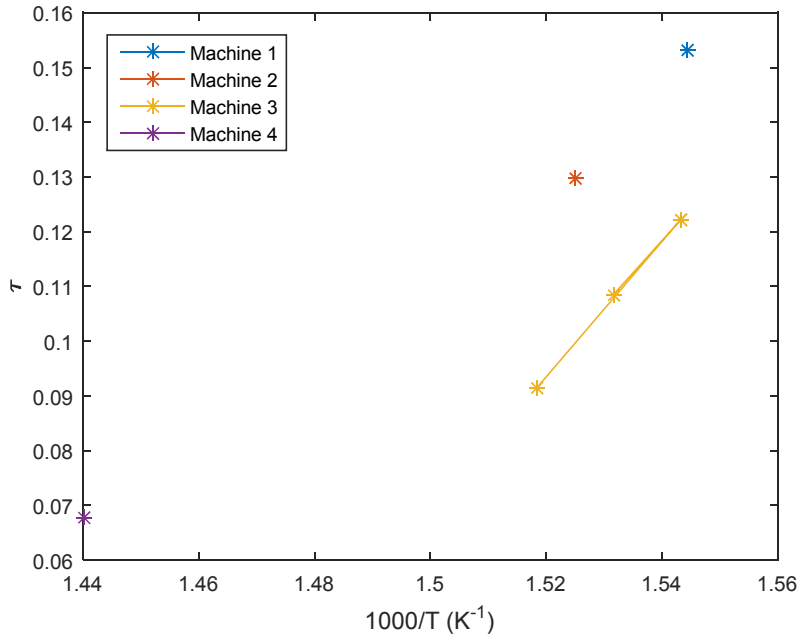

FIGURE 25: CASE 1 DATA POINT COMPARISON

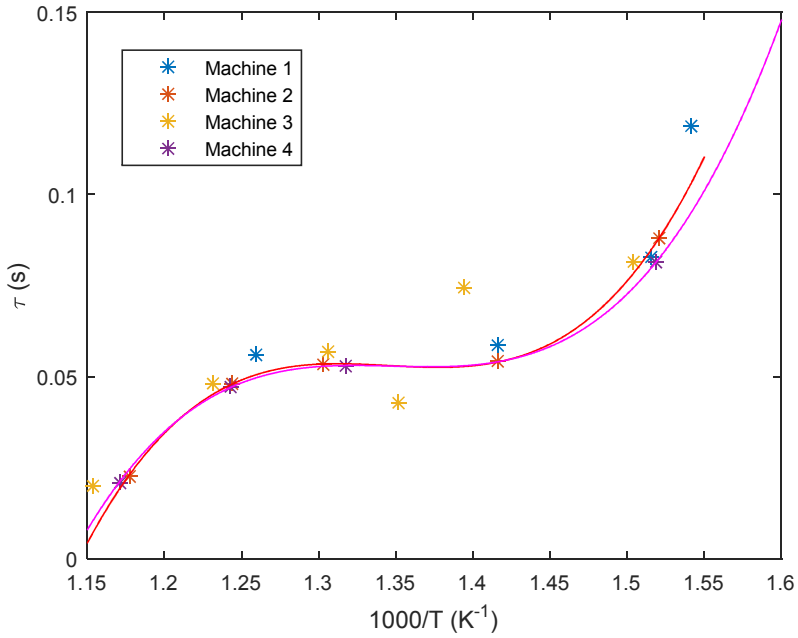

FIGURE 26: CASE 2 DATA POINT COMPARISON

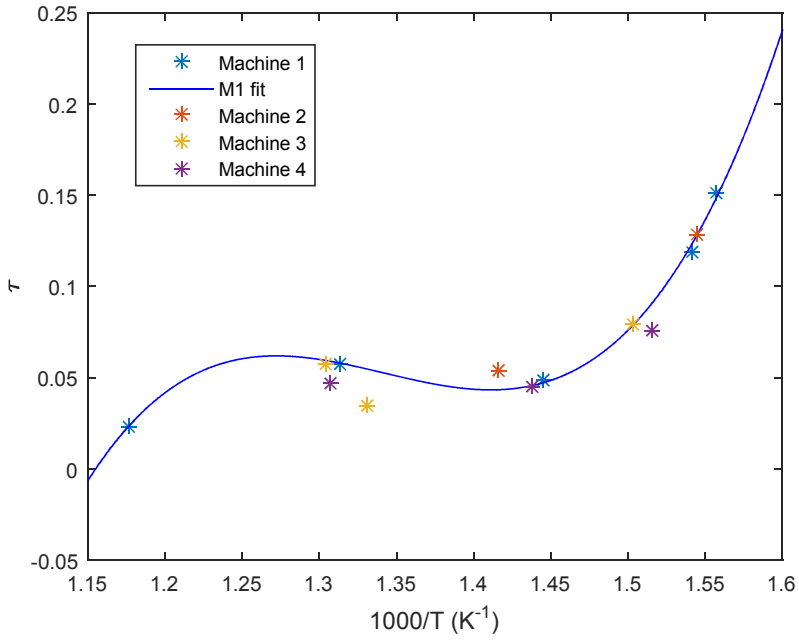

FIGURE 27: CASE 3 DATA POINT COMPARISON

Figure 25, Figure 26, and Figure 27 above depict an initial condition case comparison for each machine. Figure 25 displays the first initial condition case, which was unable to obtain many reactive cases due to the limitations of only changing the compression ratio, and not having any condition to help the temperature as discussed in Section 5.1. Figure 26 and Figure 27 have a wider variety of points due to the range that cases 2 and 3 area able to cover. Both of these initial condition cases allow for higher compressed temperatures to be reached. By pre-heating the fuel-oxidizer mixture, the compressed temperatures can be increased as well. Increasing the amount of argon in the oxidizer mixture changes the thermal properties of the mixture. This is another method that allows for an increase in the compressed temperature. Since these cases allow for an increase in the temperature of the mixture, it can be seen that this allow for a wider variety of data points. There is more of a limitation with the amount of argon in the mixture as the limitation is set to 60% due to the desired properties of the oxidizer mixture.

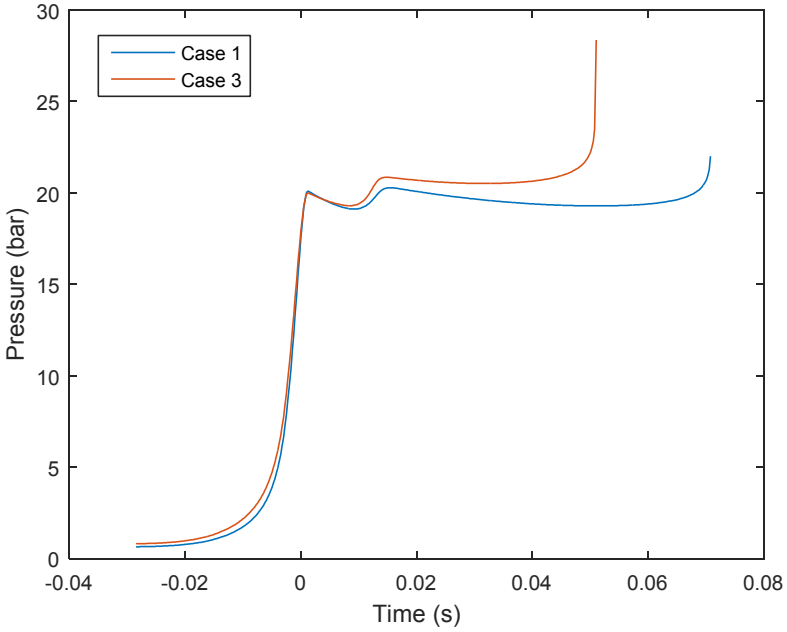

FIGURE 28: CASE 1 AND 3 PRESSURE TRACE COMPARISON

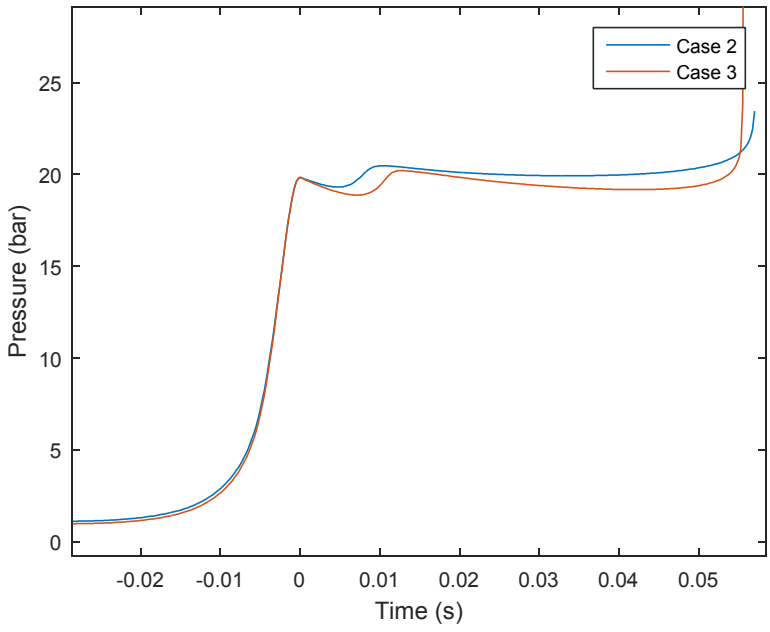

FIGURE 29: CASE 2 AND 3 PRESSURE TRACE COMPARISON

Figure 28 and Figure 29 above are taken from machine 4 and 2, respectively, as a way to determine the most influential initial condition case. It has been mentioned that the initial conditions have an effect on the data, however it is important to determine which factor is most important. Figure 28 validates previous discussion, as the case with argon present has a shorter ignition delay time than the case with only a compression ratio change. Figure 29 demonstrates how cases 2 and 3 can lead to similar conditions due to increasing the temperatures of the mixture through different methods.

Chapter 6: Conclusions and Future Work

6.1 Conclusions

Based off the results discussed in chapter 5, there were a few conclusions reached. The first of these was that, based off the machines tested, the compression time is the most influential factor when comparing datasets from different machines. By compressing the mixture more quickly, there is less of a likelihood of heat loss, which not only affects the comparison to other data sets based off that parameter, but also greatly affects the ignition delay time. In some cases, the ignition delay time for the third machine data was 20% different from the other machines, which is quite a variation. Overall, there was also more variability seen in the lower compressed temperature ranges as to be expected with longer ignition delay times as well as the susceptibility to more heat loss. The data points with compressed temperatures above 800 K were only slightly affected by the changes made to the machines and the initial conditions. The initial condition case that was determined to create the most variance was the compression ratio case. The ignition delay times for this initial condition case were significantly different from the delay times for cases 2 and 3. Some parameters varied by 4 factors in the Goldsborough paper as opposed to only 2 with the results displayed above. Overall it was determined that a variability seen within RCM datasets cannot solely be shown by changing one parameter, it is due to many parameters changing.

6.2 Future Work

Looking to what could be done to further this work, there are definitely a few efforts that could be taken. The first of these would be successfully simulating other types of machines. This may include varying the stroke length, changing the

crevice volume more substantially, or changing multiple parameters at once. With real RCM facilities, typically more than one parameter is changed when comparing facilities. The second effort to further this work would be to use multiple different initial condition cases. Changing the compression ratio as an initial condition case may be able to work over a wider range of temperatures if a higher initial temperature or a set amount of argon is used. Next, noting the specifics of experimental runs as much as possible would help in this effort, as the more information available, the more that can be done with. If facilities are able to discuss how they run their experiments or any experimental discrepancies, further efforts can be taken in this research area. Finally, it would be very helpful to examine real RCM facilities and the testing conditions they use to obtain experimental data. Having a better understanding of the exact comparison made in Figure 1 would be extremely beneficial to understand the complexities associated with RCM data.

BIBLIOGRAPHY

Goldsborough, S. S. (2009). A chemical kinetically based ignition delay correlation for iso-octane covering a wide range of conditions including the NTC region. *Combustion and Flame*, *156*(6), 1248–1262. http://doi.org/10.1016/j.combustflame.2009.01.018

Mittal, G., & Sung*, C.-J. (2007). *a Rapid Compression Machine for Chemical Kinetics Studies At Elevated Pressures and Temperatures. Combustion Science and Technology* (Vol. 179). http://doi.org/10.1080/00102200600671898

Goldsborough, S. S., Banyon, C., & Mittal, G. (2012). A computationally efficient, physics-based model for simulating heat loss during compression and the delay period in RCM experiments. *Combustion and Flame*, *159*(12), 3476–3492. http://doi.org/10.1016/j.combustflame.2012.07.010

Wilson, D., & Allen, C. (2016). Application of a multi-zone model for the prediction of species concentrations in rapid compression machine experiments. *Combustion and Flame*, *171*, 185–197. http://doi.org/10.1016/j.combustflame.2016.05.018

Wilson, D. (2016). Application of a multi-zone model for the prediction of species concentrations in rapid compression machine experiments, Marquette University.

Neuman, J. (2015). Development of a Rapid Compression Controlled-Expansion Machine for Chemical Ignition Studies, Marquette University.

Park, P., & Keck, J. C. J. (1990). *Rapid compression machine measurements of ignition delays for primary reference fuels. SAE Technical Paper Series*. Retrieved from http://papers.sae.org/900027/%5Cnhttp://dx.doi.org/10.4271/900027

Mittal, G., & Sung, C. J. (2006). Aerodynamics inside a rapid compression machine. *Combustion and Flame*, *145*(1–2), 160–180. http://doi.org/10.1016/j.combustflame.2005.10.019

Affleck, W. S., and Thomas, A. (1968). An Opposed Piston Rapid Compression Machine for Preflame Reaction Studies. Proc. Inst. Mech. Eng., 183, 365-387

Donovan, M. T., He, X., Zigler, B. T., Palmer, T. R., Wooldridge, M. S., & Atreya, A. (2004). Demonstration of a free-piston rapid compression facility for the study

of high temperature combustion phenomena, *137*, 351–365. http://doi.org/10.1016/j.combustflame.2004.02.006

Mittal, G. (2006). A Rapid Compression Machine. Case Western Reserve University

Sung, C.-J., & Curran, H. J. (2014). Using rapid compression machines for chemical kinetics studies. *Progress in Energy and Combustion Science*, *44*, 1–18. http://doi.org/10.1016/j.pecs.2014.04.001

Tanaka, S., Ayala, F., & Keck, J. C. (2003). A reduced chemical kinetic model for HCCI combustion of primary reference fuels in a rapid compression machine. *Combustion and Flame*, *133*(4), 467–481. http://doi.org/10.1016/S0010-2180(03)00057-9

Curran, H. J., Gaffuri, P., Pitz, W. J., & Westbrook, C. K. (1998). A Comprehensive Modeling Study of n -Heptane Oxidation, *2180*(97).